Ocean Dynamics (2011) 61:1937–1954
DOI 10.1007/s10236-011-0449-9

Development and testing of a coupled ocean–atmosphere mesoscale ensemble prediction system

Teddy R. Holt · James A. Cummings · Craig H. Bishop · James D. Doyle · Xiaodong Hong · Sue Chen · Yi Jin

Received: 14 January 2011 / Accepted: 2 June 2011 / Published online: 28 June 2011

Abstract A coupled ocean–atmosphere mesoscale ensemble prediction system has been developed by the Naval Research Laboratory. This paper describes the components and implementation of the system and presents baseline results from coupled ensemble simulations for two tropical cyclones. The system is designed to take into account major sources of uncertainty in: (1) non-deterministic dynamics, (2) model error, and (3) initial states. The purpose of the system is to provide mesoscale ensemble forecasts for use in probabilistic products, such as reliability and frequency of occurrence, and in risk management applications. The system components include COAMPS® (Coupled Ocean/Atmosphere Mesoscale Prediction System) and NCOM (Navy Coastal Ocean Model) for atmosphere and ocean forecasting and NAVDAS (NRL Atmospheric Variational Data Assimilation System) and NCODA (Navy Coupled Ocean Data Assimilation) for atmosphere and ocean data assimilation. NAVDAS and NCODA are 3D-variational (3DVAR) analysis schemes. The ensembles are generated using separate applications of the Ensemble Transform (ET) technique in both the atmosphere (for moving or non-moving nests) and the ocean. The atmospheric ET is computed using wind, temperature, and moisture variables, while the oceanographic ET is derived from ocean current, temperature, and salinity variables. Estimates of analysis error covariance, which is used as a constraint in the ET, are provided by the ocean and atmosphere 3DVAR assimilation systems. The newly developed system has been successfully tested for a variety of configurations, including differing model resolution, number of members, forecast length, and moving and fixed nest options. Results from relatively coarse resolution (~27-km) ensemble simulations of Hurricanes Hanna and Ike demonstrate that the ensemble can provide valuable uncertainty information about the storm track and intensity, though the ensemble mean provides only a small amount of improved predictive skill compared to the deterministic control member.

Keywords Ensembles · Coupled ocean–atmosphere modeling · Tropical cyclones · Variational analyses · Probabilistic prediction

Responsible Editor: Pierre Lermusiaux

This article is part of the Topical Collection on *Maritime Rapid Environmental Assessment*

T. R. Holt (✉) · J. A. Cummings · C. H. Bishop · J. D. Doyle · X. Hong · S. Chen · Y. Jin
Marine Meteorology Division, Naval Research Laboratory, Monterey, CA, USA
e-mail: teddy.holt@nrlmry.navy.mil

T. R. Holt · J. A. Cummings · C. H. Bishop · J. D. Doyle · X. Hong · S. Chen · Y. Jin
Oceanography Division, Naval Research Laboratory, Monterey, CA, USA

1 Introduction

All models are imperfect and all forecasts are inaccurate. Hence, at best we can hope to forecast a distribution of possible future states given our model and a history of observations. A compelling method for attempting to sample this distribution is ensemble forecasting (Toth and Kalnay 1993). The idea is to make an ensemble of forecasts whose differing initial conditions describe our best estimate of the uncertainty of the initial state estimate and whose

differing representations of sub-grid scale processes represent our uncertainty in the model. Rigorously accurate ensemble methods for describing the distribution of future states given past information include particle filters and Monte Carlo–Markov chains (Van Leeuwen 2009). Unfortunately, the computational resources required for the application of such methods to models with tens of millions of variables such as the coupled ocean–atmosphere system considered are not readily available. For this reason, computationally efficient approximations to these schemes must be used. Here we employ a framework in which the mean of the ensemble of initial conditions for the coupled ocean–atmosphere state is obtained from three-dimensional variational (3DVAR) schemes in the atmosphere and ocean and the ensemble is obtained by inputting estimates of analysis error variance from the 3DVAR data assimilation schemes into the Ensemble Transform (ET) ensemble generation technique of Bishop and Toth (1999), McLay et al. (2008), and Bishop et al. (2009).

The advent of regional two-way coupled models is relatively recent and perhaps because of this very little work has been done in the area of regional coupled model ensemble forecasting. It is, nevertheless, a very promising area of research because uncertainty in forecasts of the oceanic boundary layer is directly linked to uncertainty in forecasts of the atmospheric boundary layer (ABL) and vice versa. It is extremely difficult to model this interaction between uncertainty in the ocean and atmosphere without a coupled model. This paper represents one of the first attempts to describe this process.

A description of the components of the coupled ensemble system is given in "Section 2". "Section 3" describes the ET system, and "Section 4" details the implementation of the mesoscale ensemble system. Some basic results for two tropical cyclone (TC) case studies are provided in "Section 5" to provide a baseline for the ensemble system. We choose TC case studies because of the strong air–ocean coupling in TCs and the need for improvement in both track and intensity forecasts. While TC track forecasts have improved over the past 30 years in the Atlantic basin, with average track forecast errors reduced noticeably (Rappaport et al. 2009), it remains a critical issue to increase the accuracy of TC track forecasts in the days prior to potential landfall to provide lead time for better protection of coastal communities. In the 2008 hurricane season, Hanna and Ike were two consecutive storms that made landfall on the east and southeast coasts of the USA, respectively. The coupled ensemble system is used to simulate these two storms and make an initial assessment of system performance for both track and intensity forecasts over a 2- to 3-day period before landfall. The paper concludes with a summary and conclusions ("Section 6").

2 Description of the ocean–atmosphere coupled ensemble prediction system

The coupled system developed at the Naval Research Laboratory (NRL) is comprised of four primary components, as described in Chen et al. (2010): the nonhydrostatic atmospheric model COAMPS (Coupled Ocean/Atmosphere Mesoscale Prediction System; Hodur 1997), the hydrostatic ocean model NCOM (Navy Coastal Ocean Model; Martin 2000), the atmospheric data assimilation system NAVDAS (NRL Variational Data Assimilation System; Daley and Barker 2001a, b), and the ocean data assimilation system NCODA (Navy Coupled Ocean Data Assimilation System; Cummings 2005). A detailed description of the components is given in these references, so only a brief overview with emphasis on the new modifications to the system relevant to the ensemble implementation applied to TC applications is provided here.

2.1 COAMPS

The physical parameterizations in the atmospheric component include a cumulus parameterization (used for grid spacing greater than 10 km) based on a modified Kain–Fritsch (K–F) (Kain and Fritsch 1993; Kain 2004) scheme, a cloud microphysics scheme based on Rutledge and Hobbs (1983), and a radiation parameterization based on Harshvardhan et al. (1987). The sea surface temperature (SST) feedback is through a Monin–Obukhov-based surface similarity scheme. The surface momentum, heat, and moisture fluxes are parameterized using standard bulk aerodynamic formulae (Louis 1979):

$$U_*^2 = C_{\mathrm{D}}\overline{U}^2, \tag{1}$$

$$U_*\theta_* = C_{\mathrm{H}}\overline{U}\,\overline{\Delta\theta}, \tag{2}$$

$$U_*q_* = C_{\mathrm{E}}\overline{U}\,\overline{\Delta q}, \tag{3}$$

where U_* is the friction velocity, θ_* is the convective scaling temperature, q_* is the mixing ratio scaling, $\overline{U}$ is the mean surface wind speed, $\overline{\Delta\theta}$ and $\overline{\Delta q}$ are the mean potential temperature and vapor mixing ratio differences computed using the surface and the first model grid point above the surface (~10 m), and C_{D}, C_{H}, and C_{E} are the bulk transfer coefficients for momentum, heat, and moisture, respectively. The transfer coefficients are stability and roughness length dependent, as derived from observations, with differing momentum roughness length as compared to heat and moisture. The stability function is a modified version of Louis (1979) based on version 3.0 of the Tropical Ocean and Global Atmosphere Coupled Ocean–Atmosphere Response Experiment (TOGA COARE; Fairall et al. 2003).

Recent enhancements to several of the COAMPS physical parameterizations that reflect an increased understanding from recent TC observations and research have been made. The changes include a reduction of C_D under high winds, the inclusion of heating due to dissipation of turbulent kinetic energy (TKE), and the decrease of ice nuclei concentration to reduce upper-level cloud ice. Laboratory tank experiments suggest that C_D asymptotically approaches 2.5×10^{-3} when the surface wind speed exceeds 35 m s^{-1} (Donelan et al. 2004). This phenomenon has also been observed in wind profile measurements in TCs (Powell et al. 2003) and direct turbulence measurement at near-hurricane-force wind speeds during the latest Coupled Boundary Layers Air–Sea Transfer (CBLAST) hurricane field experiment, suggesting an even lower asymptotic value of 23 m s^{-1} (Black et al. 2007). However, the CBLAST measurements displayed a large fluctuation of C_D values for a given 10-m wind speed and had no C_D values for winds exceeding 30 m s^{-1}. Therefore, the neutral 10-m C_D over the ocean in COAMPS has been modified to be in agreement with that estimated by Donelan et al. (2004). Another change is related to heating caused by energy loss due to TKE dissipation. This process, parameterized and tested in COAMPS, shows a positive impact on TC intensity and structure forecasts (Jin et al. 2007). More recently, the ice nucleation formulation has been modified based on previous studies. This change results in better TC structure as well as intensity forecasts.

2.2 NCOM

The hydrostatic, mesoscale version of the Navy Coastal Ocean Model (NCOM) with hybrid sigma-z levels is the ocean component of the coupled system. Forcing fields from the atmospheric component are used as ocean surface boundary conditions for momentum, potential temperature, and salinity as shown by Eqs. 4–7 (Martin 2000):

$$K_M\frac{\partial u}{\partial z}=\frac{\overline{\tau_x}}{\rho_0}, \tag{4}$$

$$K_M\frac{\partial v}{\partial z}=\frac{\overline{\tau_y}}{\rho_0}, \tag{5}$$

$$K_H\frac{\partial \theta}{\partial z}=\frac{\overline{Q_b+Q_e+Q_s}}{\rho_0 c_p}, \tag{6}$$

$$K_H\frac{\partial S}{\partial z}=S(\overline{E_v}-\overline{P_r}), \tag{7}$$

where K_M and K_H are vertical eddy coefficients for the momentum and scalar fields, respectively; u and v are the horizontal components of the current fields, θ and S are the potential temperature and salinity, respectively; τ_x and τ_y are the surface wind stress in the x and y directions, respectively; Q_b, Q_e, and Q_s are the net long wave, latent, and sensible surface heat fluxes, respectively; E_v and P_r are the surface evaporation and precipitation rates, respectively; and ρ_0 and c_p are the density and specific heat for seawater, respectively. The overbars indicate time-averaged atmospheric quantities.

The atmospheric component provides a total of six fields to the ocean component, including the sea level pressure (SLP), the surface wind stress in the x and y directions (Eqs. 4 and 5), the total heat and moisture fluxes (Eqs. 6 and 7), and the net solar radiation. The net solar radiation is used to compute the diabatic heating contribution in the potential temperature equation (not shown). The SLP is also needed as input for the pressure calculations in the momentum equations of the ocean model. The coupling frequency between atmosphere and ocean is user-determined, typically on the order of 30 min or less.

2.3 NAVDAS

The NRL Atmospheric Variational Data Assimilation System (NAVDAS) is used for atmospheric data assimilation in the coupled system. NAVDAS is an observation space-based 3DVAR suite for generating maximum likelihood atmospheric state estimates to satisfy a variety of Navy needs ranging from global initial conditions for Navy global prediction to local initial conditions for forward-deployed mesoscale prediction (Daley and Barker 2001a). It is used by Fleet Numerical Meteorology and Oceanography Center (FNMOC) in the Navy Operational Global Atmospheric Prediction System (NOGAPS) and the operational mesoscale system (COAMPS) as their data assimilation schemes.

The observation space form of the 3DVAR equation is given as (Daley and Barker 2001a):

$$x_a-x_b=P_bH^T(HP_bH^T+R)^{-1}[y-\Psi(x_b)], \tag{8}$$

where x_a is the analysis, x_b the background (forecast or prior), P_b the positive-definite background error covariance matrix, H the Jacobian matrix corresponding to the (possibly) nonlinear forward or observation operator Ψ, R the observation error covariance matrix, and y the observation vector. Here x_a–x_b is the correction vector (analysis increment) and $y-\Psi(x_b)$ is the innovation vector (observation increment) of length L. The matrix to be inverted, HP_bH^T+R, is an $L\times L$ symmetric matrix. A complete description of the formulation and development of NAVDAS can be found in Daley and Barker (2001a).

NAVDAS directly assimilates a variety of observation types and off-time observations, including radiosondes and pibals, surface observations from land and sea, TIROS Operational Vertical Sounder (TOVS) radiances or temperature profiles, Aircraft Meteorological Data Reporting (AMDAR) observations and pilot reports, and Special Sensor Microwave Imager (SSM/I) surface wind speed and total precipitable water. Its formulation permits considerable local vertical and horizontal anisotropy. NAVDAS features vertical variation of the horizontal correlation scales, horizontal variation of the vertical correlation lengths, and vertical variation of the mass-divergent wind coupling.

NAVDAS interfaces with NOGAPS (global) and COAMPS (regional) through the correction vectors that are produced for the grid of that model. For the multiple nested-grid COAMPS, the same set of observations is used for all nests but the characteristics of the background error covariance vary between the outer grid and the innermost nest. The observation innovation is computed from the highest resolution background field and the analysis grid is constructed by removing any duplicate grid points from the COAMPS grid meshes. An additional correction is added to the outer grid meshes to account for differences between the background forecasts in the grid meshes (Sashegyi et al. 2009).

One of the advantages in using NAVDAS in the global or regional ensemble forecast system is that it produces estimates of the error variance of its analyses. Such variance estimates can be used to constrain the magnitude of initial perturbations that represent ET transformations or linear combinations of ensemble forecast perturbation (Bishop and Toth 1999). It overcomes the drawback of the multivariate optimum interpolation (MVOI) scheme used in earlier tests of the COAMPS ensemble prediction system since the MVOI scheme does not produce estimates of the analysis error variance (Bishop et al. 2009; Holt et al. 2009).

NAVDAS analysis error variance estimates are used in the ET scheme for the NRL global ensemble prediction system and results show that the generated ET analysis perturbations exhibit statistically significant, realistic multivariate correlations. The forecast ensembles are comparable to or better in a variety of measures than those produced by FNMOC bred-growing modes scheme (McLay et al. 2008). Even the NAVDAS analysis error variance generated from the global model and interpolated for the mesoscale ensemble prediction system is able to produce reasonable ET analysis perturbations (Bishop et al. 2009; Holt et al. 2009).

2.4 NCODA

The ocean data assimilation component of the coupled ensemble forecast system is the Navy Coupled Ocean Data Assimilation (NCODA) system. NCODA is a fully multivariate 3DVAR system that provides simultaneous analyses of five ocean variables: temperature, salinity, geopotential, and u- and v-vector velocity components. The horizontal correlations are multivariate in geopotential and velocity, thereby permitting adjustments to the mass fields to be correlated with adjustments to the flow fields. The velocity adjustments (or increments) are in geostrophic balance with the geopotential increments, which in turn are in hydrostatic agreement with the temperature and salinity increments. NCODA corrects ocean model initial conditions using a sequential incremental update cycle. It has been cycled with a variety of ocean forecast models, including HYCOM (HYbrid Coordinate Ocean Model) and NCOM, which are in operational use at the Navy forecasting centers. The system can be run global or regional, where it supports relocatable, multi-scale analyses on nested higher-resolution grids using a 3:1 nested grid ratio. This nesting strategy is of particular importance in Navy applications where very high resolution is required in a rapid environmental assessment mode of operation.

NCODA assimilates a wide variety of ocean observation data types including satellite SST retrievals (AATSR, AMSR-E, METOP-AVHRR, GOES, MSG, MTSAT, NOAA-AVHRR), sea ice concentration retrievals (SSM/I, SSMIS), fixed, drifting buoy, and ship in situ SSTs; temperature and salinity profiles (Argo, CTD casts, fixed and drifting buoys, gliders, expendable bathythermographs); satellite altimeter sea surface height anomalies (ENVISAT, GFO, Jason, Topex); significant wave height retrievals from altimeters and wave buoys; and velocity observations (HF radar, surface drifters, acoustic Doppler current profilers, gliders, and Argo trajectories). NCODA is tightly coupled to a fully automated ocean data quality control system that is executed in real time at the Navy centers (Cummings 2011).

NCODA is an oceanographic implementation of the NAVDAS algorithm and solves the observation space form of the 3DVAR in the ocean using Eq. 8. A specification of the background and observation error covariances in the analysis is very important. Background error covariances are separated into an error variance and a correlation. The correlations are separated further into horizontal and vertical components. Horizontal correlation length scales vary with location and are set proportional to the first baroclinic Rossby radius of deformation (Chelton et al. 1998), which varies from ~10 km at the poles to ~200 km at the equator. Flow dependence is introduced by modifying horizontal correlations with a tensor that takes into account the geopotential height separation between observations and grid locations. The flow dependence spreads model data differences along, rather than across, geopotential contours such as ocean fronts and eddies. Vertical correlation length scales are computed by scaling a specified change in density stability criterion with background

vertical density gradients according to:

$$h_v = \rho_s/(\partial\rho/\partial z) \tag{9}$$

where h_v is the vertical correlation length scale, ρ_s is the specified change in density criterion (~0.12 kg m^{-3}), and $\partial\rho/\partial z$ is the local vertical density gradient. The resulting vertical correlation length scales vary with location and depth and are large (small) when the water column stratification is weak (strong). Vertical correlations are updated based on the forecast valid at the analysis time. In this way, the vertical scales evolve from one analysis cycle to the next and capture changes in mixed layer and thermocline depths.

Background error variances are derived from a time history of the analysis increment fields and a model variability component derived from a time history of model forecast differences according to:

$$e_b = \sum_{j=1}^{m} w_j (x_j - x_{j-1})^2 + \sum_{j=1}^{m} \tau \cdot \alpha_j^2 \tag{10}$$

where e_b is the background error variance, j is the update cycle, m is the number of update cycles into the past, w_j is a weight computed from a geometric time series, $w_j=(1-\phi)^{j-1}$, where ϕ is a tunable constant between 0 and 1 (typically set to 0.1), (x_j–x_{j-1}) is the difference between successive forecasts, α_j is the analysis increment field, and τ is a correlation time scale computed from a ratio of the spatially varying horizontal length scales h and forecast velocity fields v valid at the analysis time, $\tau=e^{-(h/v)}$. The weights are normalized such that the weighted averages of the two components are unbiased. Subscripts depicting 3D position coordinates have been eliminated for clarity. The time scales vary with location and depth and range from days near the surface in the western boundary current regions to years at depth in the tropical ocean where current speeds are slow and length scales are large. In this approach, model data errors tend to dominate the background error variance estimates in low-flow environments, while model variability tends to dominate in high-flow (i.e., hurricane-induced) environments. Background error variances are computed for all of the model prognostic variables and updated at each analysis update cycle.

3 Description of the Ensemble Transform technique

The ET ensemble generation technique transforms an ensemble of forecast perturbations into an ensemble of analysis perturbations that are consistent with a user-provided estimate of the analysis error covariance matrix $\mathbf{P}^a$. Assume that there are n model variables in total (typically, $n \sim O(10^7)$) and K ensemble members in total (typically, $K \sim O(10) - O(10^2)$). Let the columns of the $n \times K$ matrix $\mathbf{X}^f$ list the forecast perturbations about the forecast ensemble mean all valid at the time of the most recent analysis. Let the columns of the n x K matrix $\mathbf{X}^a$ denote the analysis perturbations that will be added to the most recent analysis to create an ensemble of initial conditions consistent with the accuracy of the most recent analysis. The ET transforms $\mathbf{X}^f$ into $\mathbf{X}^a$ using:

$$\mathbf{X}^a = \mathbf{X}^f \mathbf{T}, \tag{11}$$

As noted in McLay et al. (2008), to compute the required transformation matrix one first performs the eigenvector decomposition:

$$\frac{\mathbf{X}^{fT}\mathbf{P}^{a-1}\mathbf{X}^f}{n} = \mathbf{C}\Lambda\mathbf{C}^T, \tag{12}$$

where the orthonormal $K \times K$ matrix $\mathbf{C}$ lists the orthonormal eigenvectors of $\mathbf{X}^{fT}\,\mathbf{P}^{a-1}\,\mathbf{X}^f/n$ and the diagonal matrix Λ lists the corresponding eigenvalues. Because the sum of the forecasts perturbations is zero, one of the eigenvalues will always be equal to zero. The eigenvector corresponding to this eigenvalue is always parallel to the vector $\mathbf{1}^T = \overbrace{[1,1,...,1]}^{K-\text{elements}}$ where $\mathbf{1}$ is a column vector of ones. For the reasons discussed in McLay et al. (2008), a new diagonal matrix A is created from Λ by replacing the zero eigenvalue by the unity. The transformation matrix is then given by:

$$\mathbf{T} = \mathbf{C}A^{-1/2}\mathbf{C}^T, \tag{13}$$

When $\mathbf{T}$ is defined in this way, the analysis perturbations obtained from Eq. 11 satisfy the equation:

$$\frac{\mathbf{X}^{aT}\mathbf{P}^{a-1}\mathbf{X}^a}{n} = \mathbf{I} - \frac{\mathbf{1}\mathbf{1}^T}{K}, \tag{14}$$

where $\mathbf{I}$ is a $K \times K$ identity matrix. As noted in McLay et al. (2008), Eq. 14 implies that (1) the analysis perturbations are quasi-orthogonal under the analysis error covariance norm and (2) if the ensemble size K was large enough to satisfy $K=n$, then the sample covariance of the analysis perturbations would equal the prescribed analysis error covariance matrix $\mathbf{P}^a$. Note that Eq. 11 means that the analysis perturbations are just linear combinations of forecast perturbations. Hence, if the forecast perturbations lie in the space of growing balanced perturbations, then the analysis perturbations will also. Indeed Eq. 11 means that the ET ensemble generation technique may be viewed as an advanced form of Toth and Kalnay's (1993) breeding technique with added constraints of quasi-orthogonality and fit to the prescribed analysis error covariance matrix $\mathbf{P}^a$.

In its purest form, only one set of transformation coefficients is used for the entire state. However, McLay et al. (2010) have shown that smoothly blending the

transformation coefficients relevant to large regions such as the tropics and extra-tropics can lead to performance advantages. In this first study, we approximate Eq. 12 for both the atmospheric and oceanic components and apply separate transformation coefficients for the atmosphere and the ocean.

For the ocean component, NCODA includes options to estimate the analysis error variance defined as the reduction of forecast error from assimilation of the observations. Similar to the description of NAVDAS above ("Section 2.3") the primary application of the NCODA analysis error variance is in the oceanic ET technique. The ocean ET is multivariable and is computed for temperature, salinity, and velocity simultaneously. In warm start mode, the ocean ET operates identical to the atmosphere ET (see "Section 4" for a discussion of cold start and warm start modes of the coupled system). However, in cold start mode, the ocean ET is limited by two factors: (1) there is no forecast error product from the deterministic global NCOM (gNCOM) and (2) there is no global NCOM ensemble from which to draw the initial set of perturbations. To solve this problem in cold start mode, we treat a time series of gNCOM forecasts at the update cycle interval as members of an ensemble. The number of members used in the actual ensemble determines how far back in time we have to obtain gNCOM fields. The NCODA analysis background error variances and the initial perturbations for the ensemble are initialized from this time series. This process results in NCODA analysis background error variances and ET perturbations that are multivariate, balanced, and consistent. The ability to relocate the coupled system for rapid environmental assessment is thereby enhanced as well.

4 Implementation of the mesoscale ensemble system

The components of the ocean–atmosphere coupled system as described in "Section 3" are efficiently integrated into an ensemble framework under the Earth System Modeling Framework as illustrated in Fig. 1. A basic differential starting point for the ensemble system is a "cold start" versus a "warm start." The specifics of each, and their differences, are described here.

A cold start is executed initially and only once for a given case study. The first module executed in the system is the analysis, indicated by the upper box in Fig. 1a. Because this is the initial execution of the mesoscale system, there are no previous "background" (BKG) forecasts to be used as first guesses for the analysis. Thus, global fields must be used. The control member is the only ensemble member to execute the analysis (step 1 in Fig. 1). The analysis consists of two basic parts: preparing the observations, initial conditions (IC), boundary conditions (BC), and BKG fields for (1) the atmosphere and (2) for the ocean. The atmospheric analysis is based on NAVDAS (see "Section 2.3"), using the control member from the 33-member (32 members plus control) Navy Operational Global Atmospheric Prediction System (NOGAPS) ensemble run at T119 horizontal resolution (~110 km) and 30 vertical levels, interpolated to the COAMPS atmospheric domain as

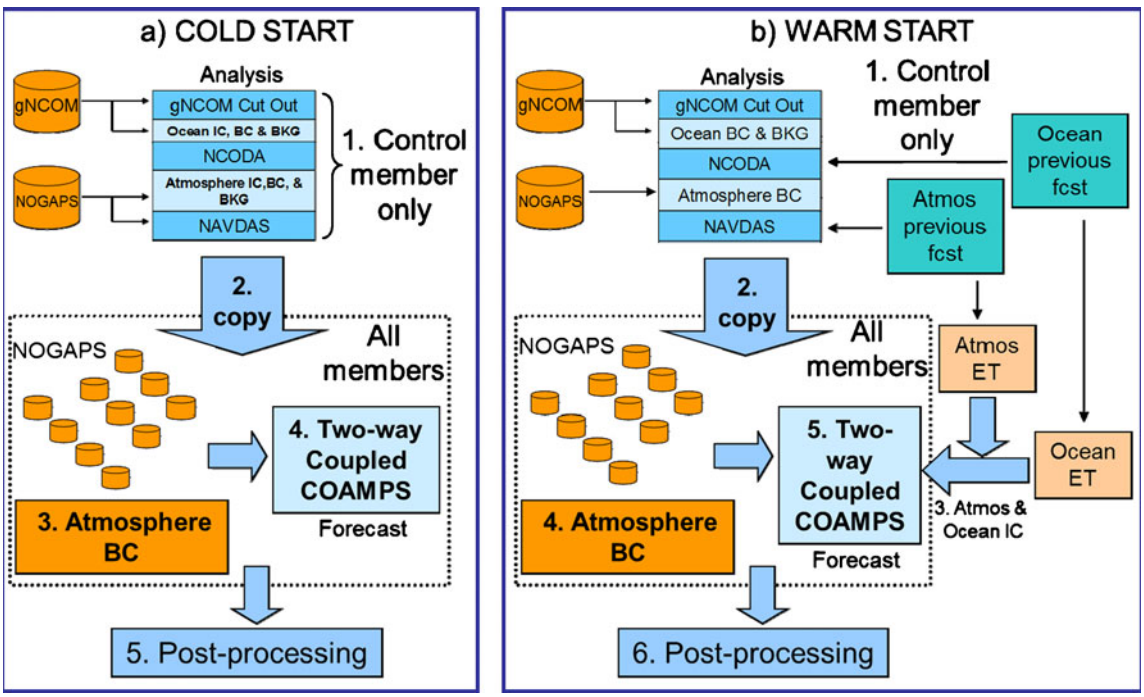

Fig. 1 Schematic showing the implementation of the air–ocean coupled ensemble system for **a** a cold start and **b** a warm start

the first guess. The oceanic analysis is based on NCODA (see "Section 2.4"), using gNCOM interpolated to the COAMPS oceanic domain as first guesses. There is currently no global ocean ensemble, so the deterministic run is used.

The analyzed atmospheric and oceanic output fields from the control member are next copied to all members (step 2). Each member now creates unique atmospheric lateral BC from 28 members of the global NOGAPS ensemble (step 3). The members of the global ensemble are produced using perturbation methodology based on the banded ET as described in McLay et al. (2008, 2010). The banded ET produces initial perturbations by transforming 6-h ensemble forecast perturbations to be consistent with analysis error estimates. The local banded ET performs this transformation in latitude bands, resulting in a better match to the analysis error estimate, and much improved performance in the mid-latitudes, as compared to the global ET computed over the entire globe. Stochastic kinetic energy backscatter (Shutts and Palmer 2004; Shutts 2005; Berner et al. 2009) is planned for future implementations of the ET adopted to account for model uncertainty and increase in size of tropical perturbations. Step 4 is to execute the coupled forecast model for each of the members, using the same initial conditions but different lateral atmospheric BC, followed by post-processing (step 5).

The implementation of the ensemble system for a warm start differs from a cold start in several ways (Fig. 1b). First, though the analysis is again executed only for the control member (upper box in Fig. 1b), the BKG fields for both NAVDAS and NCODA are previous control member forecasts (typically 6 or 12 h) from the ensemble (not global fields). The analysis creates and copies the same fields as for the cold start (step 2). However, the IC for the individual members are now obtained by adding the ET perturbations to the control analysis (see "Section 3"), separate for both the

Table 1 Listing of the atmospheric physics options and perturbations. Italicized values for the members (1–28) indicate values that differ from the control (member 0; see text for a detailed description of the physics parameters)

Member	abl	mixlen	Flux	w-kf	tinc-lcl	cld-rad	precip	Graupel	Auto-conv	Rain-int	Snow-int
0 (control)	2	1.0	1.0	1.0	0.0	1,500.0	0.0	True	0.0004	8.0e6	2.0e7
1 (PBL buoyancy)	*1*	1.0	1.0	1.0	0.0	1,500.0	0.0	True	0.0004	8.0e6	2.0e7
2 (PBL mixing length)	2	*1.25*	1.0	1.0	0.0	1,500.0	0.0	True	0.0004	8.0e6	2.0e7
3 (PBL mixing length)	2	*0.75*	1.0	1.0	0.0	1,500.0	0.0	True	0.0004	8.0e6	2.0e7
4 (PBL mixing length)	2	*1.5*	1.0	1.0	0.0	1,500.0	0.0	True	0.0004	8.0e6	2.0e7
5 (PBL mixing length)	2	*0.5*	1.0	1.0	0.0	1,500.0	0.0	True	0.0004	8.0e6	2.0e7
6 (PBL surface flux)	2	1.0	*1.25*	1.0	0.0	1,500.0	0.0	True	0.0004	8.0e6	2.0e7
7 (PBL surface flux)	2	1.0	*0.75*	1.0	0.0	1,500.0	0.0	True	0.0004	8.0e6	2.0e7
8 (PBL surface flux)	2	1.0	*1.5*	1.0	0.0	1,500.0	0.0	True	0.0004	8.0e6	2.0e7
9 (PBL surface flux)	2	1.0	*0.5*	1.0	0.0	1,500.0	0.0	True	0.0004	8.0e6	2.0e7
10 (cumulus W trigger)	2	1.0	1.0	*1.5*	0.0	1,500.0	0.0	True	0.0004	8.0e6	2.0e7
11 (cumulus W trigger)	2	1.0	1.0	*0.5*	0.0	1,500.0	0.0	True	0.0004	8.0e6	2.0e7
12 (feedback fraction)	2	1.0	1.0	1.0	0.0	1,500.0	*0.5*	True	0.0004	8.0e6	2.0e7
13 (cumulus T trigger)	2	1.0	1.0	1.0	*1.0*	1,500.0	0.0	True	0.0004	8.0e6	2.0e7
14 (cumulus T trigger)	2	1.0	1.0	1.0	*-1.0*	1,500.0	0.0	True	0.0004	8.0e6	2.0e7
15 (cumulus T trigger)	2	1.0	1.0	1.0	*2.0*	1,500.0	0.0	True	0.0004	8.0e6	2.0e7
16 (cumulus T trigger)	2	1.0	1.0	1.0	*-2.0*	1,500.0	0.0	True	0.0004	8.0e6	2.0e7
17 (cloud radius)	2	1.0	1.0	1.0	0.0	*500.0*	0.0	True	0.0004	8.0e6	2.0e7
18 (cloud radius)	2	1.0	1.0	1.0	0.0	*1,000.0*	0.0	True	0.0004	8.0e6	2.0e7
19 (cloud radius)	2	1.0	1.0	1.0	0.0	*2,000.0*	0.0	True	0.0004	8.0e6	2.0e7
20 (cloud radius)	2	1.0	1.0	1.0	0.0	*3,000.0*	0.0	True	0.0004	8.0e6	2.0e7
21 (feedback fraction)	2	1.0	1.0	1.0	0.0	1,500.0	*1.0*	True	0.0004	8.0e6	2.0e7
22 (graupel)	2	1.0	1.0	1.0	0.0	1,500.0	0.0	*False*	0.0004	8.0e6	2.0e7
23 (microphysics)	2	1.0	1.0	1.0	0.0	1,500.0	0.0	True	*0.00004*	8.0e6	2.0e7
24 (microphysics)	2	1.0	1.0	1.0	0.0	1,500.0	0.0	True	*0.004*	8.0e6	2.0e7
25 (microphysics)	2	1.0	1.0	1.0	0.0	1,500.0	0.0	True	0.0004	*8.0e7*	2.0e7
26 (microphysics)	2	1.0	1.0	1.0	0.0	1,500.0	0.0	True	0.0004	*8.0e5*	2.0e7
27 (microphysics)	2	1.0	1.0	1.0	0.0	1,500.0	0.0	True	0.0004	8.0e6	*2.0e8*
28 (microphysics)	2	1.0	1.0	1.0	0.0	1,500.0	0.0	True	0.0004	8.0e6	*2.0e6*

Table 2 Description of the TC case studies. The number of forecasts indicates the number of data assimilation forecasts executed every 12 h for the case study. Ike-u is the same as Ike except that the atmospheric model was run uncoupled with the ocean model

Case	Cold start date	No. of forecasts	Members	Atmos resolution (km)	Ocean resolution (km)	Atmospheric levels	Ocean levels	Forecast length (h)	Moving nests	Coupled
Hanna	2008090112	6	29	81, 27	27	30	40	54	Y	Y
Ike	2008090500	14	29	81, 27	27	30	40	60	Y	Y
Ike-u	2008090500	14	29	81, 27	27	30	40	60	Y	N

atmosphere and the ocean (step 3). The lateral boundary conditions are created the same as for a cold start (step 4) as are the execution of the forecast model (step 5) and post-processing (step 6). The entire process (from step 1 to 6) is repeated for the next data assimilation cycle.

Previous simulations testing the ensemble system displayed tendencies for the forecast to be under-dispersive (too little spread). To address this issue and to better represent uncertainty, atmospheric perturbations are developed and tested as described in the following section.

4.1 Atmospheric perturbations

In order to represent the uncertainty due to the model physical parameterizations, each of the COAMPS members is run with a different set of physical parameterization values as shown in Table 1. Previous COAMPS ensemble experiments were conducted with a variety of atmospheric parameters. The results from these experiments isolated several key parameters in the ABL and cumulus parameterizations and cloud microphysics to which COAMPS forecasts were most sensitive. The parameterization developers were consulted in order to focus on a subset of key parameters that they thought represented the largest uncertainty. These parameters are: (1) the type of ABL parameterization, (2) the magnitude of the vertical mixing length, (3) the magnitude of the surface sensible and latent heat fluxes, (4) the grid-scale vertical velocity used in the K–F cumulus parameterization trigger for convective initiation, (5) the fraction of available convective precipitation partitioned to the grid-scale precipitation, (6) the temperature increment at the lifted condensation level (LCL) (which also impacts the convective initiation in the K–F parameterization), (7) the cloud updraft radius used in the K–F parameterization, (8) microphysical interactions that include graupel, (9) the microphysics auto-conversion factor, and (10) the microphysics slope intercept factors for snow and rain. A brief description for each is given here.

1. The ABL parameterization: Ensemble member 1 uses the original Mellor and Yamada (1974, 1982) ABL scheme (abl=1). The modified Mellor and Yamada boundary layer scheme (abl=2) has several features not

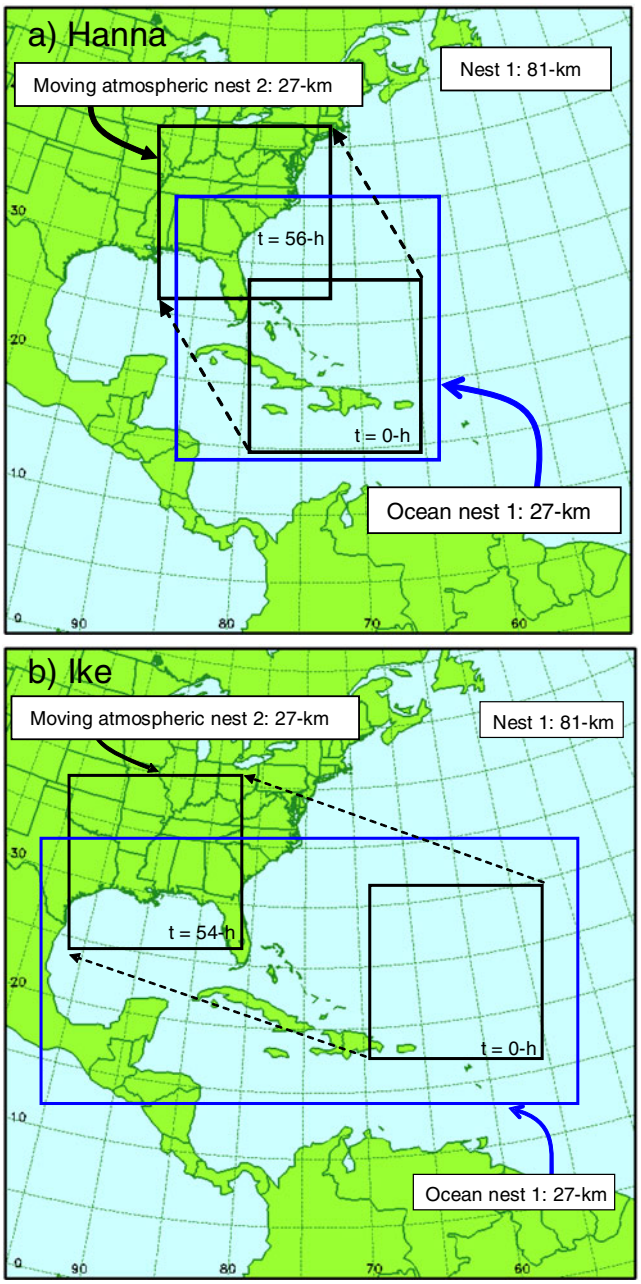

Fig. 2 The coupled model domain setup for the TC case studies: **a** Hanna and **b** Ike (see Table 2 for details on each configuration)

available in the original formulation. A statistical cloud fraction is computed for the buoyancy calculation. This is used in diagnosing the virtual buoyancy flux which impacts the buoyant production of turbulence. The thermodynamic quantities used for determining stability include liquid water potential temperature and a hybrid potential temperature incorporating both liquid water potential temperature and virtual potential temperature. All five species of water substance (vapor, liquid, snow, ice, and graupel) are used in all thermodynamic computations. The use of these quantities removes the discontinuity at cloud base which was a common occurrence in the original Mellor and Yamada scheme. In terms of shear production, a background shear based on the turbulence level is included as the lower limit on shear production of TKE. The turbulence length scale is modified to increase more rapidly with elevation in highly convective situations. In addition, the Brunt–Vaisala length scale used in stable conditions is not utilized within cloud layers. The modified ABL scheme is used for all members except ensemble member 1 (see Table 1).

2. The magnitude of the vertical mixing length: COAMPS uses separate vertical eddy mixing coefficients for momentum, K_M:

$$K_M = S_M l_V e^{-1/2}, \tag{15}$$

and for the scalar variables, K_H:

$$K_H = S_H l_V e^{-1/2}, \tag{16}$$

where l_V represents the vertical mixing length, S_M and S_H the stability factors for momentum and scalars, and e the TKE (Mellor and Yamada 1974; Therry and Lacarrère 1983). This vertical mixing length is scaled by factor *mixlen* (ranging from 0.5 to 1.5) for perturbation members 2–5.

3. The magnitude of the surface sensible and latent heat fluxes: The sensible and latent fluxes as given by Eqs. 2 and 3 are scaled by factor *flux* (ranging from

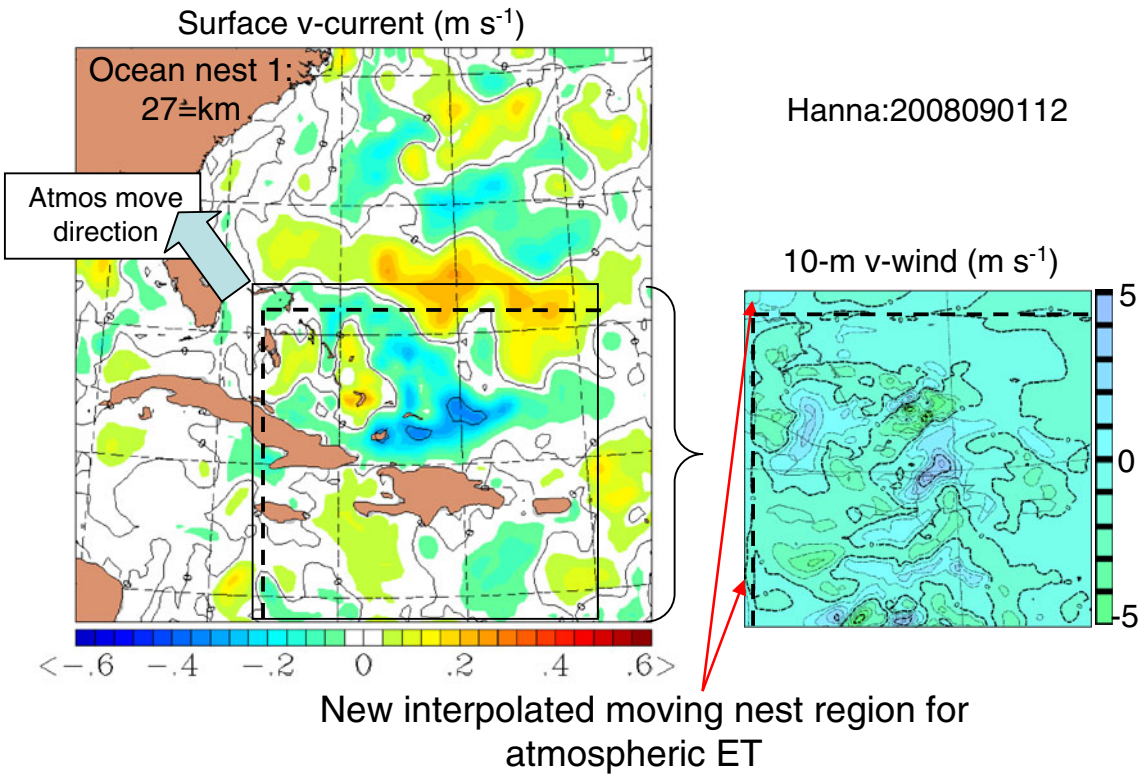

Fig. 3 The ocean nest 1 (27 km) analyzed surface v-current (m s^{-1}) and the location of the atmospheric nest 2 (27 km) for the control member (*solid box*) and member 1 (moved nest indicated by *dashed lines*) for the 1200 UTC 1 September Hurricane Hanna case (*left*) and the analyzed nest 2 (27 km) 10-m wind v-component (m s^{-1}) after the moving nest ET algorithm has been applied (*right*)

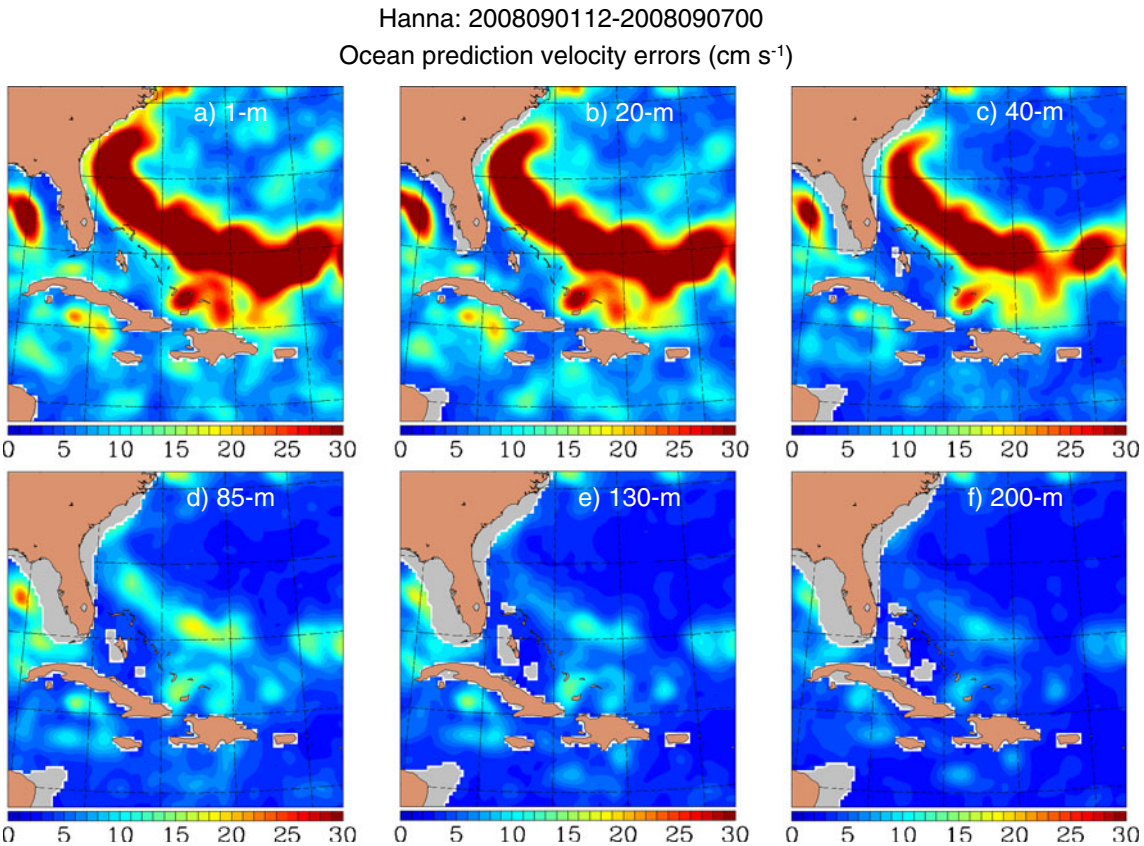

Fig. 4 Ocean prediction velocity errors (cm s^{-1}) for ocean nest 1 (27-km) for Hurricane Hanna averaged from 1200 UTC 1 September to 0000 UTC 7 September for depths **a** 1 m, **b** 20 m, **c** 40 m, **d** 85 m, **e** 130 m, and **f** 200 m

0.5 to 1.5) over land and water for perturbation members 6–9.

4. The grid-scale vertical velocity used in the K–F cumulus parameterization to diagnose convective initiation: The value is scaled by factor *w-kf* (ranging from 0.5 to 1.5) for members 10 and 11.
5. The fraction of available convective precipitation that is partitioned to the grid-scale precipitation: The value is scaled by factor *precip* (ranging from 0.5 to 1.0) for members 12 and 21.
6. The temperature increment at the LCL: The increment (*K*) added to the temperature at the LCL (*tinc-lcl*) ranges from −2.0 to 2.0 K for members 13–16. This increment has an impact on the convective initiation.
7. The cloud updraft radius used in the K–F parameterization: The radius *cld-rad* (m) varies from 500 to 3,000 m for members 17–20.
8. Graupel: Graupel microphysics calculations (*graupel*) are not included for member 22.
9. Microphysics auto-conversion factor: The cloud water mixing ratio threshold in the Kessler (1969) auto-conversion of cloud water to rain (*auto-conv*) varies from 0.00004 to 0.004 for

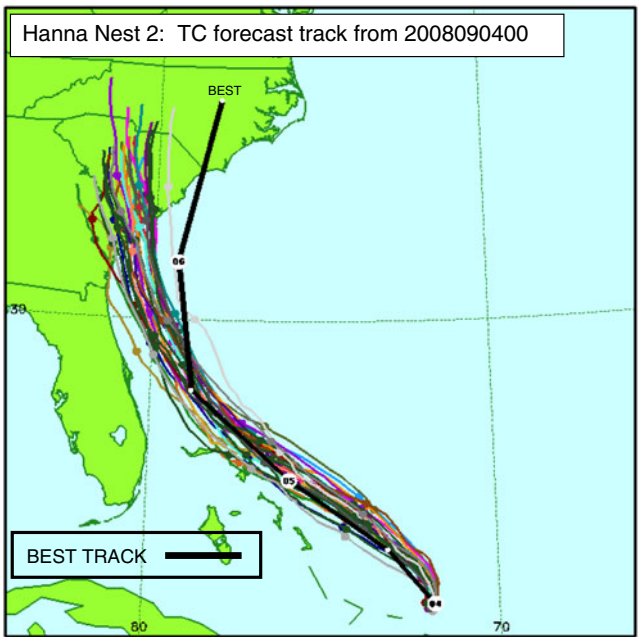

Fig. 5 TC forecast tracks for 29-member Hurricane Hanna for the warm start at 0000 UTC 4 September for 0 to 54 h for the COAMPS coupled ensemble. The *white circles* on the best track indicate the day (04, 05, 06), and the *solid circles* for the forecast tracks are every 12 h. (Note that the member number colors are not consistent for the map and the error statistics are given in Fig. 6)

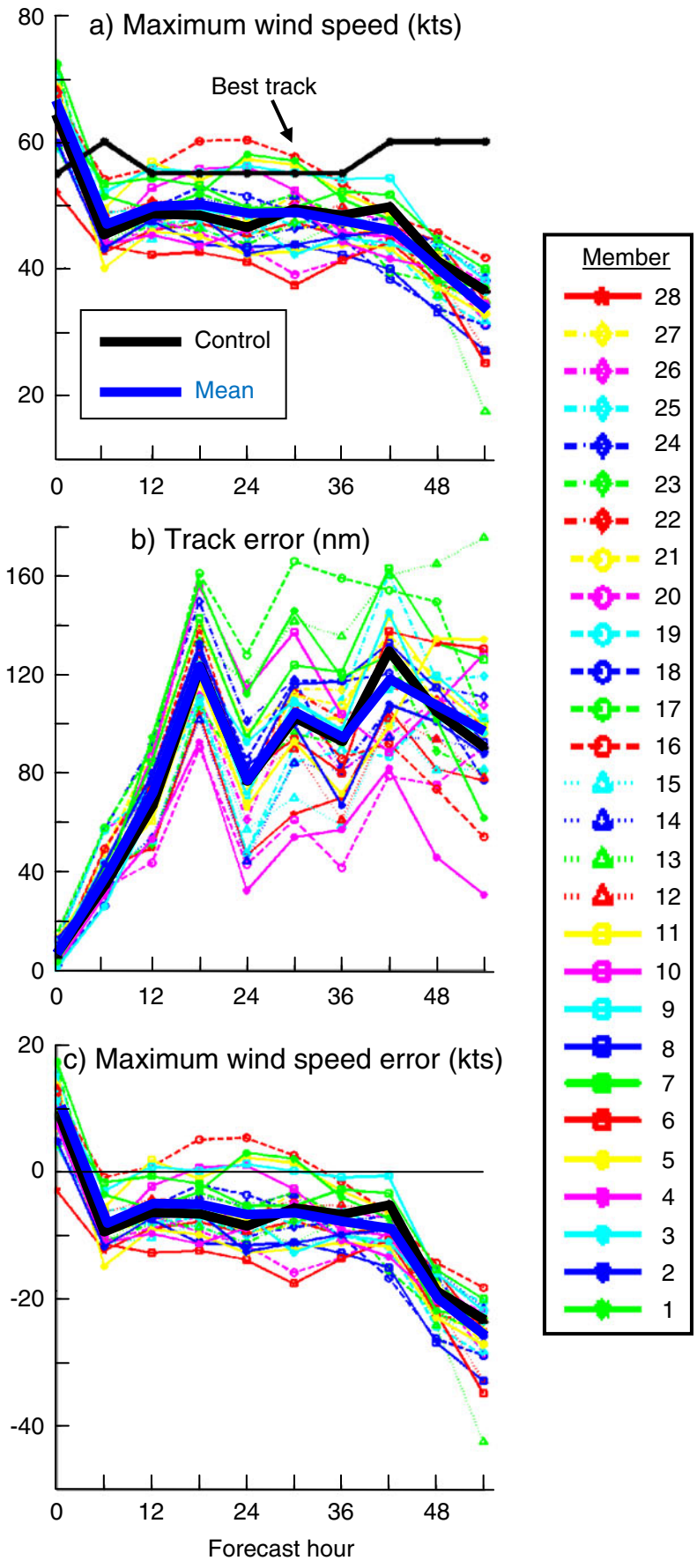

Fig. 6 COAMPS coupled ensemble statistics for 29-member Hurricane Hanna for the warm start at 0000 UTC 4 September for 0 to 54 h of **a** maximum wind speed (kts), **b** track error (nm), and **c** maximum wind speed error (kts). The control forecast is given by the *thick black line*, and the ensemble mean is given by the *thick blue line*. The wind speed from the observed best track TC is given by the *solid line*. (Note that the member number colors are not consistent for the map in Fig. 5 and the error statistics)

members 23 and 24. There is no conversion unless cloud water mixing ratio > *auto-conv*.

10. Microphysics slope intercept factors: The intercept factors for the raindrop size (*rain-int*) vary from 8.e5 to 8.e7 for members 25 and 26 and snow flake size (*snow-int*) distributions vary from 2.e6 to 2.e8 for members 27 and 28.

5 Results of tropical cyclone case studies

Coupled ensemble simulations are conducted for two TC case studies: Hanna (1–6 September 2008) and Ike (5–14 September 2008). The primary focus of this study is to demonstrate the capability of the coupled ensemble system not to provide high-resolution simulations of the TCs. Thus, the following analyses stress the performance of the coupled ensemble (particularly the ensemble mean versus the deterministic control forecast) and not the detailed high-resolution validation against observations.

Hurricane Hanna is investigated over the period from 1 to 6 September 2008. However, the storm was prominent as early as 28 August when it was named. By 30 August, the circulation was weak, centered near its location just east of the Bahamas. Hurricane Gustav's circulation influenced Hanna's track on 1 September, causing a slow drift to the south-southwest with convection and strong intensification, with the National Hurricane Center (NHC) upgrading Hanna to a hurricane (sustained winds of at least 64 kts or 33 m s^{-1}). However, Gustav again impacted Hanna's structure and by 2 September strong wind shear weakened the circulation and the storm was downgraded to a tropical storm on 3 September. Hanna made landfall near the South Carolina–North Carolina border on 6 September and subsequently went extra-tropical by 7 September.

Hurricane Ike is investigated over the period from 5 to 14 September 2008. Ike was a very long-lived system, first evident in the Atlantic as Tropical Depression Nine on 1 September, with several subsequent periods of intensification and weakening over the next 10 days. Ike reached peak intensity (~145 kts or 79 m s^{-1}) by 4 September, weakened to category 3 on 5 September and category 2 on 6 September. This weakening was short-lived and rapid intensification occurred again in the early hours of 7 September, reaching category 4 (with sustained winds of 115 kts near the Caicos Islands) just 6 hours after being downgraded to category 2. Ike made several landfalls at Caribbean islands on 8 and 9 September before rapidly intensifying during the night of 10 September (reduction in central SLP from 963 to 944 hPa and increase in wind speed from 74 to 87 kts) as it passed over the loop current in the Gulf of Mexico. From 10 to 12 September, Ike remained a category 2 storm (~95 kts) as it moved north-northwestward toward Galveston, TX, USA, but with an unusually large spatial distribution of high wind speeds, resulting in a large storm surge as it made landfall at ~0700 UTC 13 September.

A variety of configurations, including differing model resolution, number of members, forecast length, and moving and fixed nest configurations, have been tested for the coupled ensemble system. A "standard" configuration is chosen for the two TC cases presented here, as listed in Table 2 and shown in Fig. 2. Each of the studies begins with a cold start (as described in "Section 4"), employs data assimilation every 12 h, and uses atmospheric model

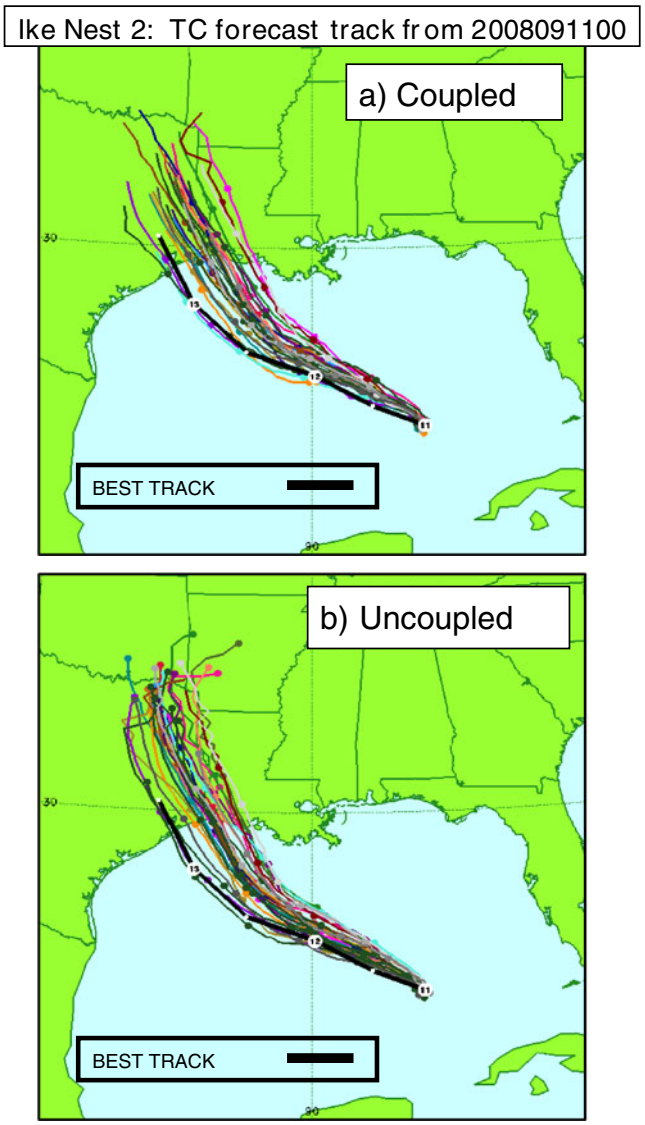

Fig. 7 TC forecast tracks for 29-member Hurricane Ike for the warm start at 0000 UTC 11 September for the COAMPS **a** coupled ensemble and **b** uncoupled ensemble. The tracks correspond to different forecast lengths (60 and 72 h) than the best track (*solid black*). The *white circles* on the best track indicate the day (11, 12, 13) and the *solid circles* for the forecast tracks are every 12 h

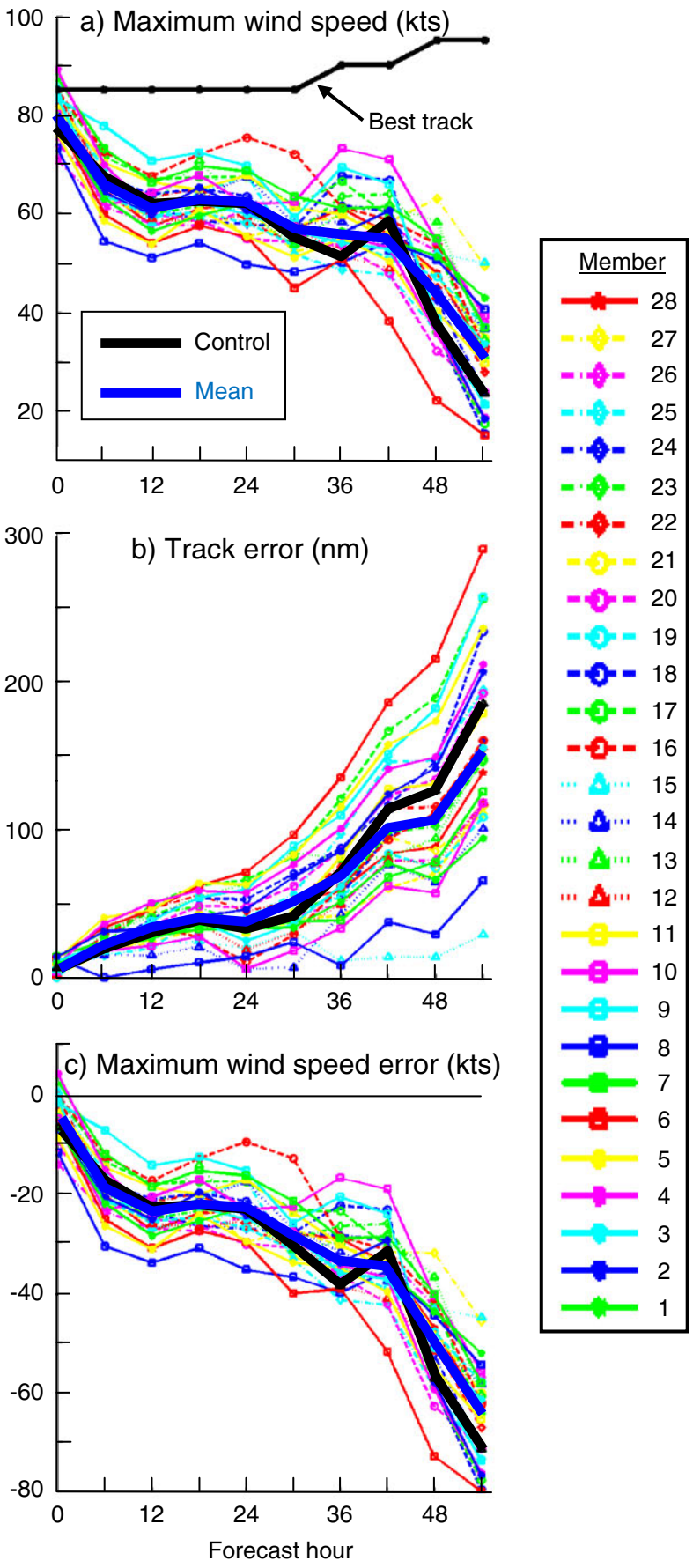

Fig. 8 COAMPS coupled ensemble statistics for 29-member Hurricane Ike for the warm start at 0000 UTC 11 September for 0 to 54 h, similar to Fig. 6

perturbations (as outlined in "Section 4.1"), with a two-way exchange of information every time step between the grid meshes. The Hanna case study cold start begins at 1200 UTC 1 September 2008 (Ike at 0000 UTC 5 September 2008), with a series of 54-h (60-h for Ike) forecasts every 12 h for 3 days or six total forecasts (7 days or 14 forecasts for Ike). The ensemble simulations use two atmospheric domains with a horizontal resolution of 81 and 27 km, with the second nest moving automatically with the TC center, and one fixed ocean domain with 27-km resolution. The atmospheric model has 30 vertical levels with the vertical grid spacing varied from 10 m near the surface to a maximum of 7,500 m near the model top (~30 km). The ocean model has 40 vertical levels, including 19 terrain-following sigma levels in the upper 140 m and 21 fixed-depth levels between 140 m and the ocean bottom. The Ike case study is also simulated with the atmospheric model uncoupled to the ocean model (*Ike-u*) in addition to the standard coupled configuration.

For TC applications in which the inner nests of the atmospheric model may move with the TC, there is an inherent problem in implementing the ET to create a new initial state because it cannot be guaranteed that the model domains of every member will coincide spatially. In fact, it is a desired result for none of the members to coincide, such that the TC track of each member is different to enable the spread to better represent the natural variability. For the application of the ET, this results in a spatially inconsistent background field. Thus, a new capability to apply the ET for moving nests has been developed. The new algorithm is described below.

For a given BKG field (i.e., 12-h forecast), the spatial area for each member that is common with the control member (i.e., overlap region) is computed. Then, for each individual member, that area of the moving nest which is outside the overlap region is interpolated from the domain of the parent (i.e., if nest 2 is the moving nest, then nest 1 would be the parent used for interpolation). This new domain that is now the same as the control domain is used as the BKG field for the ET. Figure 3 shows an example of the implementation of the algorithm for the 1200 UTC 1 September 2008 Hanna case. The atmospheric domain for the control member is given by the solid box in the right corner of the ocean nest 1 (27 km) surface v-current (left panel). The moving nest member has moved to the northwest following the TC, so the new interpolated region encompasses a region to the north and west of the control domain, indicated by the dashed line. The new atmospheric 10-m v-wind component, including the interpolated region, is given in the right panel. Note that the interpolated region contains only weak gradients. The amount of discontinuity will obviously depend upon the difference in the model solution on the parent and child domains in the interpolated region. In addition, the smaller the overlap region of different member domains (i.e., the larger the interpolated regions), the larger the potential adverse impact on the ensemble mean because of increased interpolation.

Figure 4 shows the NCODA 3DVAR ocean velocity BKG errors for the Hurricane Hanna case study averaged from 1200 UTC 1 September to 0000 UTC 7 September. As discussed in "Section 2.4," there are two components of the BKG error: model variability and model data errors. Model variability is dependent on the time history of forecast differences at the updated cycle interval (12 h), and model data errors are determined by the time history of the analyzed increment fields. As a result, NCODA 3DVAR BKG errors adapt as the ocean model evolves over time due to changes in the atmospheric forcing and initial conditions from the assimilation. The characteristics of the ocean prediction errors of temperature and salinity (not shown) have similar features as ocean velocity. For hurricane-

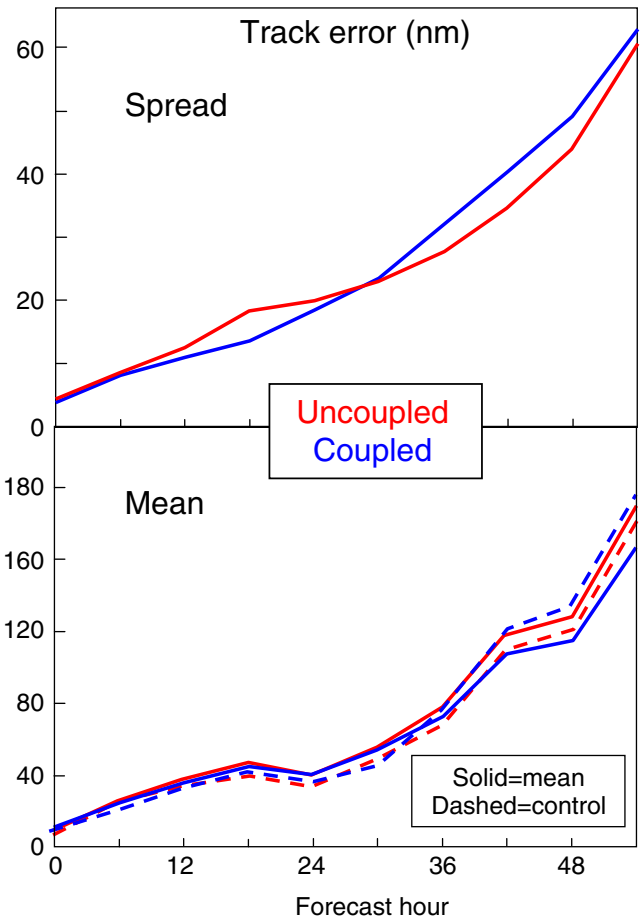

Fig. 9 Mean and spread track statistics for 29-member Hurricane Ike (coupled) and Ike-u (uncoupled) simulations for 0000 UTC 11 September. The track error values are plotted to 54 h to correspond approximately to landfall time

induced high-flow regimes, Fig. 4 shows that the horizontal distribution of the ensemble mean ocean velocity BKG errors within the ocean mixed layer is mainly in the vicinity of the envelope of ensemble tracks near the hurricane maximum winds.

On 4 September, Hanna moved out of a counter-clockwise looping motion over the Caicos Island and began to move northwestward (Fig. 5). Hanna turned northward 24 to 36 h later along the western edge of a now better established subtropical ridge over the Atlantic. The intensity of Hanna remained basically unchanged, around 55–60 kts during this period (Fig. 6a). In general, the ensemble mean forecast track for Hanna follows the best track closely for the first 36 h but, over the next 18 h, shifts to the west of the best track as the storm separates from an upper-level low pressure system and is influenced by the westward extension of the ridge. A similar deviation of the forecast track is also evident in the NOGAPS forecasts (not shown). The ensemble mean track errors (Fig. 6b) at 24, 36, and 48 h are well within the average errors for the official NHC forecasts of Hanna [1 nautical mile (nm) = 1.852 km]. The ensemble forecasts show average intensity errors of <10 kts for the period prior to landfall (Fig. 6c), while official forecasts over-estimate Hanna as a category-2 storm upon landfall. Furthermore, the ensemble mean of intensities captures the steady intensity period (not always an easy task for mesoscale models), influenced by the effect of ocean cooling in the coupled system. The ensemble mean and control forecasts are similar for both track and intensity, with only small variations for different forecast times. Though the ensemble mean is not a significant improvement over the control, the ensemble does provide the possibility for uncertainty information about the track and intensity.

The forecast tracks for Hurricane Ike are shown in Fig. 7. Both coupled and uncoupled ensemble simulations are performed to examine the impact of air–sea coupling on the track and intensity of the hurricane. The uncoupled simulation is conducted in an identical manner to the coupled simulation with the exception that there is no feedback between the ocean and atmosphere. Thus, the analyzed SST computed from NCODA is held fixed in time for the 60-h forecasts for the 14 uncoupled ensemble simulations. Generally, the forecast tracks for the time

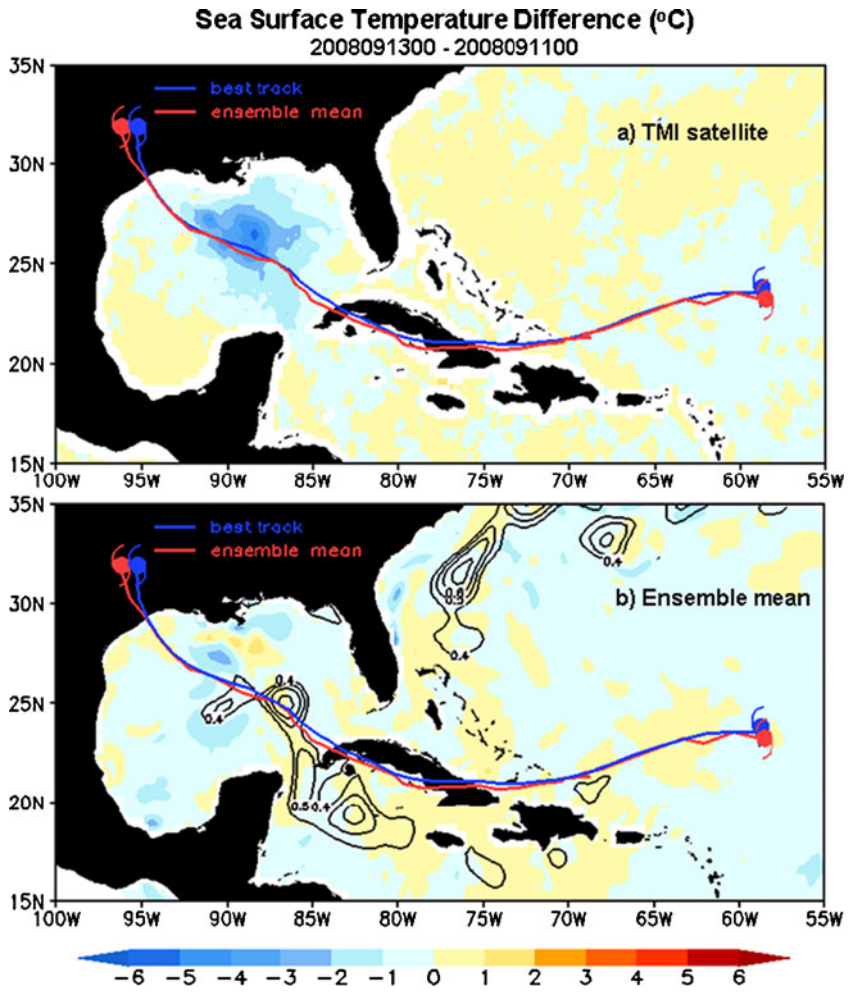

Fig. 10 Sea surface temperature difference (°C) from 0000 UTC 11 September to 0000 UTC 13 September for Hurricane Ike for **a** TRMM Microwave Imager satellite observations and **b** coupled ensemble mean. The contours in **b** are sea surface height to show the location of the warm core eddy in the Gulf of Mexico. Only surface heights greater than 0.4 m are drawn. The ensemble mean track is computed from the 0- to 11-h average forecast position

period 0000 UTC 11 September to 0000 UTC 13 September for both coupled and uncoupled simulations are similar, with the majority of tracks to the right of best track. The ensemble statistics for the coupled simulation (Fig. 8) clearly indicate that this coarse resolution simulation is unable to capture the intensity of the observed hurricane prior to landfall (wind speed errors ~20–40 kts; SLP errors ~25–40 hPa not shown). A comparison of the control and the ensemble mean indicates that the ensemble mean performs no worse and slightly better than the control in predicting track and intensity (i.e., at 48 h, mean track error = 105 vs. 125 nm for control). The use of the coupled model (versus the uncoupled) has a general positive impact on track (Fig. 9). The coupled ensemble mean track error is generally smaller than the uncoupled track error (i.e., 48-h uncoupled track error = 120 nm) and the spread is generally larger (48-h coupled ensemble spread = 53 vs. 45 nm for uncoupled).

Improvements would be expected at higher resolutions relative to this coarse resolution (27 km). It should be noted that high resolution (~5 km or less) (Chen et al. 2007) is typically required for mesoscale models to provide any skill in forecasting TC intensity. The Hanna and Ike cases provide some indication that the ensemble system can be a useful tool to improve TC track and intensity forecasts, even at a relatively coarse resolution.

Figure 10 shows the SST difference between 0000 UTC 11 September and 0000 UTC 13 September for Hurricane Ike for the TRMM Microwave Imager satellite observations and the coupled ensemble mean. There is a warm core eddy (WCE) in the Gulf of Mexico located near 25° N, 87° W as indicated by the sea surface height contours in Fig. 10b. Observations show a significant SST change on the right side of the storm track after Ike passes the WCE with SST decreased by up to ~4°C over 48 h. The ensemble mean shows a similar location for the SST decrease but with a smaller magnitude (~2°C). The area of cooling in the ensemble mean is also smaller. The difference of temperature change between the observations and the ensemble mean is consistent with a much weaker forecasted storm intensity as compared to the best track (Fig. 8a). The lack of intensity could certainly account for the weaker cooling, although Hong et al. (2000) surmise that the weaker cooling could be related to modifications in the pre-storm ocean thermal structure as a result of changes in vertical mixing. The lack of cooling indicates that the upper ocean stratification is not strong enough to represent the pre-storm conditions.

During the life cycle of a TC, the region along the TC track should also be a region of large ensemble spread. Figure 11 shows the ensemble spread for Hurricane Ike for the 24-h forecast valid 1200 UTC 11 September of surface wind stress and surface current. The ensemble spread of the surface wind stress is maximum in the relatively large region of high TC wind speeds and relatively small outside the region. Likewise, the spread of the surface current is a maximum in the core TC region, with larger values emanating out from the center to the north-northeast in a clockwise spiral. The region of large spread to the northwest of the Yucatan Peninsula is believed to be due to an ocean

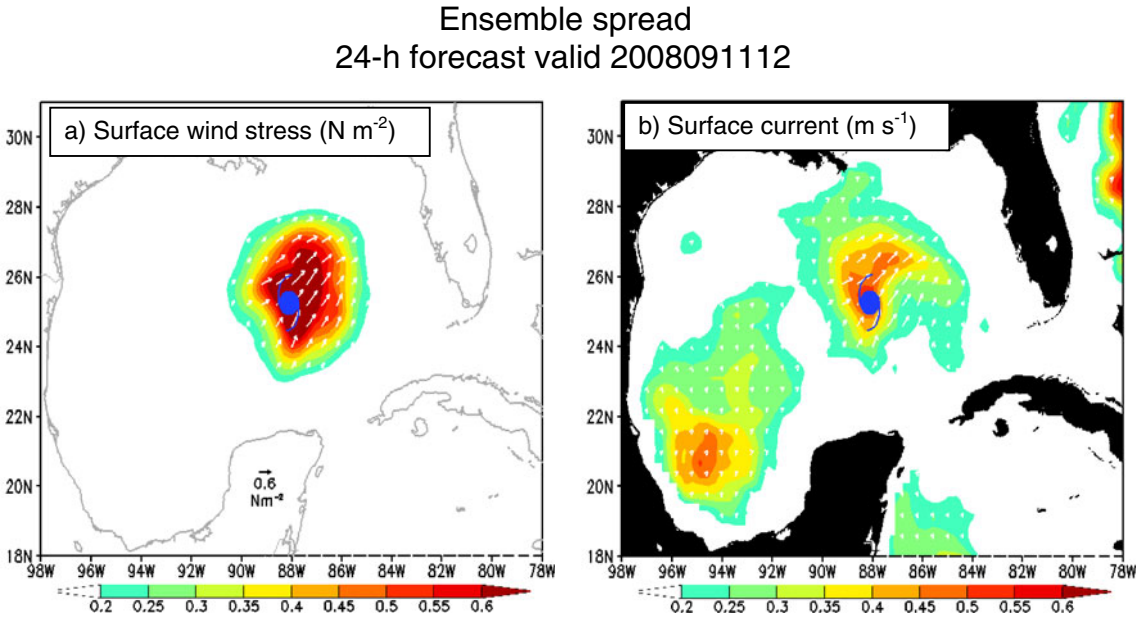

Fig. 11 Ensemble spread for the 29-member Hurricane Ike case for the 24-h forecast valid 1200 UTC 11 September of **a** surface wind stress (N m^{-2}) and **b** surface current (m s^{-1})

eddy in several ensemble members and is believed to be spurious. Spread-skill relationships of atmosphere and ocean temperature forecasts at various levels for both Hanna and Ike (not shown) further support the under-dispersive nature of the ensemble system, indicating a general lack of spread among ensemble members. This is a common feature of most ensemble systems (Houtekamer and Mitchell 2001), and improved techniques are being developed to improve the spread, particularly in the ocean, and will be presented in a follow-on paper.

6 Summary and conclusions

The development and testing of a coupled ocean–atmosphere mesoscale ensemble prediction system has been described. The system components include COAMPS and NCOM for atmosphere and ocean forecasting and NAVDAS and NCODA for 3D variational atmosphere and ocean data assimilation. The components are efficiently implemented under the Earth System Modeling Framework and have been rigorously tested for a variety of model configurations and case studies. The Ensemble Transform technique is currently used independently for the ocean (current, temperature, and salinity variables) and atmosphere (wind, temperature, and moisture variables) to create perturbations for the coupled system. Estimates of analysis error covariance from the ocean and atmosphere 3DVAR assimilation systems are used to constrain the ET.

Results are presented for tropical cyclone case studies of Hanna and Ike (September 2008) to demonstrate the baseline capability of the system. A suite of atmospheric perturbations are used to represent the uncertainty due to the model physical parameterizations (see Table 1). Generally, the ensemble mean has comparable skill as compared to the deterministic control member for hurricane track and intensity (even at a relatively coarse 27-km resolution). For Hanna, the ensemble mean forecast track errors from 0 to 48 h are well within the average errors for the official forecasts prior to landfall. The average forecast intensity error among members is ~10 kts for the period prior to landfall, while the official NHC forecasts over-estimated Hanna as a category-2 storm upon landfall. The average forecast intensity error among members for Ike (~20–40 kts) is greater than for Hanna as both the coupled and uncoupled systems did not initialize the storm sufficiently well (initial errors at 0000 UTC 11 September of ~30 hPa). Both the ocean and atmosphere components of the ensemble are under-dispersive. Efforts are underway to improve the spread, particularly in the ocean.

Future plans for the system include the development of ensemble ocean–atmosphere coupled covariances using innovative localization techniques. This approach will enable ensemble 4D-variational (4DVAR) coupled data assimilation. The ensemble 4DVAR system will provide improved state estimates of the coupled system and increase the effectiveness of ensemble-based targeted observation approaches that are currently limited by spurious ensemble correlations and by neglected error correlations between atmosphere and ocean variables. New case studies with the updated system are proposed for both TC and non-TC cases to investigate and quantify the skill of the coupled ensemble system at higher spatial resolutions. It is envisioned that the new updated system will provide improved mesoscale ensemble forecasts for use in probabilistic products, such as reliability and frequency of occurrence, and in risk management applications.

Acknowledgements This work was funded by project support from the Oceanographer of the Navy through the program office at PEO C4I PMW-120 (PE 0603207 N). Special thanks to Carolyn Reynolds and Justin McLay of NRL for providing the global ensemble data.

References

Berner J, Shutts GJ, Leutbecher M, Palmer TN (2009) A spectral stochastic kinetic energy backscatter scheme and its impact on flow-dependent predictability in the ECMWF ensemble prediction system. J Atmos Sci 66:603–626

Bishop CH, Toth Z (1999) Ensemble transformation and adaptive observations. J Atmos Sci 56:1748–1765

Bishop CH, Holt T, Nachamkin J, Chen S, McLay J, Doyle J, Thompson WT (2009) Regional ensemble forecasts using the Ensemble Transform technique. Mon Wea Rev 137:288–298

Black PG et al (2007) Air–sea exchange in hurricanes: synthesis of observations from the coupled boundary layer air–sea transfer experiment. Bull Amer Meteor Soc 88:357–374

Chelton DB, DeSzoeke RA, Schlax MG, Naggar KE, Siwertz N (1998) Geographical variability of the first baroclinic Rossby radius of deformation. J Physical Oceanogr 28:433–460

Chen SS, Zhao W, Donelan MA, Price JF, Walsh EJ (2007) The CBLAST-hurricane program and the next-generation fully coupled atmosphere–wave–ocean models for hurricane research and prediction. Bull Amer Meteor Soc 88:311–317

Chen S, Campbell TJ, Jin H, Gabersek S, Hodur RM, Martin P (2010) Effect of two-way air–sea coupling in high and low wind speed regimes. Mon Wea Rev 138:3579–3602

Cummings JA (2005) Operational multivariate ocean data assimilation. Quart J Roy Meteor Soc 131:3583–3604

Cummings JA (2011) Ocean data quality control. In: Operational oceanography in the 21st century. Springer (in press)

Daley R, Barker E (2001a) NAVDAS source book 2001: the NRL atmospheric variational data assimilation system. NRL Publication NRL/PU/7530-00-418, 160 pp. [available from Marine Meteorology Division, NRL, Monterey, CA 93943-5502]

Daley R, Barker E (2001b) NAVDAS: formulation and diagnostics. Mon Wea Rev 129:869–883

Donelan MA, Haus BK, Reul N, Plant WJ, Stiassnie M, Graber HC (2004) On the limiting aerodynamic roughness of the ocean in very strong winds. Geophys Res Lett 31:L18306. doi:10.1029/2004GL019460

Fairall C, Bradley E, Hare J, Grachev A, Edson J (2003) Bulk parameterization of air–sea fluxes: updates and verification for the COARE algorithm. J Climate 16:571–591

Harshvardhan, Davies R, Randall DA, Corsetti TG (1987) A fast radiation parameterization for atmospheric circulation models. J Geophys Res 92:1009–1016

Hodur RM (1997) The Naval Research Laboratory's Coupled Ocean/Atmosphere Mesoscale Prediction System (COAMPS). Mon Wea Rev 125:1414–1430

Holt T, Pullen J, Bishop CH (2009) Urban and ocean ensembles for improved meteorological and dispersion modeling of the coastal zone. Tellus 61A:232–249

Hong X, Chang SW, Raman S, Shay LK, Hodur R (2000) The interaction between hurricane Opal (1995) and a warm core ring in the Gulf of Mexico. Mon Wea Rev 128:1347–1365

Houtekamer PL, Mitchell HL (2001) A sequential ensemble Kalman filter for atmospheric data assimilation. Mon Wea Rev 129:123–137

Jin Y, Thompson WT, Wang S, Liou C-S (2007) A numerical study of the effect of dissipative heating on tropical cyclone intensity. Wea Forecasting 22:950–966

Kain JS (2004) The Kain–Fritsch convective parameterization: an update. J Appl Meteor 43:170–181

Kain JS, Fritsch JM (1993) Convective parameterization for mesoscale models: the Kain–Fritsch scheme. The representation of cumulus convection in numerical models. *Meteorol. Monogr.*, 24, Amer. Meteor. Soc., Boston, pp 165–170

Kessler E (1969) On the distribution and continuity of water substance in atmospheric circulations. *Meteorol. Monogr.*, 10, Amer. Meteor. Soc., Boston, p 88

Louis J-F (1979) A parametric model of vertical eddy fluxes in the atmosphere. Bound-Layer Meteor 17:187–202

Martin PJ (2000) Description of the NAVY coastal ocean model version 1.0. NRL Rep. NRL/FR/7322-00-9962, 42 pp

McLay J, Bishop CH, Reynolds CA (2008) Evaluation of the Ensemble Transform analysis perturbation scheme at NRL. Mon Wea Rev 136:1093–1108

McLay J, Bishop CH, Reynolds CA (2010) A local formulation of the Ensemble Transform (ET) analysis perturbation scheme. Wea Forecasting 25:985–993

Mellor G, Yamada T (1974) A hierarchy of turbulence closure models for planetary boundary layers. J Atmos Sci 31:1791–1806

Mellor G, Yamada T (1982) Development of a turbulence closure model for geophysical fluid problems. Rev Geophys Space Phys 20:851–875

Powell MD, Vickery RJ, Reinhold TA (2003) Reduced drag coefficient for high wind speeds in tropical cyclones. Nature 422:279–283

Rappaport EN, Franklin JL, Avila LA, Baig SR, Beven JL, Blake ES, Burr CA, Jiing JG, Juckins CA, Knabb RD, Landsea CW, Mainelli M, Mayfield M, McAdie CJ, Pasch RJ, Sisko C, Stewart SR, Tribble AN (2009) Advances and challenges at the National Hurricane Center. Wea Forecasting 24:395–419

Rutledge SA, Hobbs PV (1983) The mesoscale and microscale structure and organization of clouds and precipitation in midlatitude cyclones. VIII: a model for the "seeder–feeder" process in warm-frontal rainbands. J Atmos Sci 40:1185–1206

Sashegyi K, Pauley PM, Frost MD, Geiszler DA (2009) Hourly analyses with NAVDAS 3DAR system for COAMPS-OS, 16th Conference on Satellite Meteorology and Oceanography, 10–15 January 2009. Available at: http://ams.confex.com/ams/89annual/techprogram/paper_146820.htm

Shutts G (2005) A kinetic energy backscatter algorithm for use in ensemble prediction systems. Quart J Roy Meteor Soc 131:3079–3102

Shutts G, Palmer TN (2004) The use of high-resolution numerical simulations of tropical circulation to calibrate stochastic physics schemes. Proc. ECMWF/CLIVAR simulation and prediction of intra-seasonal variability with emphasis on the MJO, Reading, UK, European Centre for Medium-Range Weather Forecasts, pp 83–102

Therry G, Lacarrère P (1983) Improving the kinetic energy model for planetary boundary layer description. Bound-Layer Meteor 25:63–88

Toth Z, Kalnay E (1993) Ensemble forecasting at NMC: the generation of perturbations. Bull Amer Meteor Soc 74:2317–2330

Van Leeuwen PJ (2009) Particle filtering in geophysical systems. Mon Wea Rev 137:4089–4114